Quantum Error Correction on a D-Wave Quantum Annealer using 3-repetition code

Muhammad Ubaid Ur Rehman

May 2025

Abstract

We investigate the impact of error-mitigation and error-correction techniques on solving the NP-hard Max-Cut problem with a D-Wave Advantage-5.4 QPU. Using a 50-node Erdős–Rényi graph, we benchmark a raw sampling baseline, built-in spin-reversal (gauge) transforms, and a custom three-repetition encoding with majority-vote decoding. Gauge transforms deliver only a modest boost over the raw baseline, whereas the Rep-3 encoding consistently yields a markedly better cut quality and lower chain-break rate. Mild parameter tuning (longer anneal windows and stronger chain strengths) further amplifies the benefit of Rep-3, highlighting a clear trade-off: lightweight built-ins give incremental gains at no qubit cost, while logical repetition offers substantial accuracy improvements at the price of increased resources.

Quantum computing holds the promise of exponentially expanding computational power, opening new frontiers in physics, chemistry, secure communications, and beyond. Yet that potential remains out of reach because today's devices are highly susceptible to noise and decoherence. Quantum error correction (QEC) encompasses the protocols and algorithms designed to suppress or mitigate these detrimental effects. Robust QEC is the key prerequisite for transforming quantum computing from a laboratory curiosity into a scalable, industry-grade technology capable of tackling real-world problems.

1 Quantum Annealing Fundamentals

Quantum annealing (QA) is a computing paradigm designed to locate low-energy configurations of an Ising or QUBO cost function by letting a quantum-mechanical system physically relax toward its ground state. Instead of executing a sequence of logic gates, the device realizes a time-dependent Hamiltonian that interpolates between a simple transverse-field driver and the user-programmed problem Hamiltonian.

1.1 Problem Hamiltonian

A quadratic unconstrained binary optimisation (QUBO) problem is mapped to an Ising Hamiltonian

$$H_P = \sum_{i=1}^{N} h_i \, \sigma_i^z + \sum_{i<j} J_{ij} \, \sigma_i^z \sigma_j^z, \tag{1}$$

where $\sigma_i^z = |0\rangle \langle 0|_i - |1\rangle \langle 1|_i$ and h_i, J_{ij} are programmable biases and couplers.

1.2 Annealing Schedule

The time-dependent Hamiltonian implemented on-chip is

$$H(t) = A(t)H_D + B(t)H_P, \qquad 0 \le t \le t_f, \tag{2}$$

with driver term $H_D = -\sum_i \sigma_i^x$. Functions $A(t)$ and $B(t)$ satisfy $A(0) \gg B(0)$ and $A(t_f) \ll B(t_f)$. For sufficiently slow total anneal time t_f, the adiabatic theorem ensures the system remains near its instantaneous ground state. Standard schedules span 1–200 μs on *Advantage* devices.

1.3 Read-out

At $t = t_f$, a dc-SQUID measurement collapses each qubit to $|0\rangle$ or $|1\rangle$. Repeating the anneal 10^3–10^4 times yields a distribution of candidate solutions.

1.4 Sources of Errors

A Thermal Noise and Excitations

During a quantum anneal the processor is held at a finite base temperature—about 20 mK on current D-Wave systems—so the qubits couple not only to the time-dependent Hamiltonian $H(t)$ but also to a thermal bath. *Thermal noise* drives stochastic single-spin and multi-spin excitations; whenever the instantaneous gap $\Delta(t)$ between the ground and first–excited state approaches $k_{\mathrm{B}}T$, the bath can repopulate excited levels and thus reduce the probability of finishing the anneal in the true ground state.

B Intrinsic Control Error (ICE)

Calibration granularity and line crosstalk yield systematic deviations δh_i, δJ_{ij}, effectively perturbing H_P and biasing solutions.

$$E^{\delta}_{\mathrm{ising}}(\mathbf{s}) \;=\; \sum_{i=1}^{N} \big(h_i + \delta h_i\big)\, s_i \;+\; \sum_{i=1}^{N} \sum_{j=i+1}^{N} \big(J_{i,j} + \delta J_{i,j}\big)\, s_i s_j,$$

C Flux Noise

$1/f$ magnetic fluctuations in Josephson junctions dephase the qubits and broaden the minimum gap.

D Chain Breaks in Minor Embeddings

Due to limitations of QPU topology, logical variables often require *chains* of ferromagnetically coupled physical qubits (minor embedding). Insufficient chain strength κ leads to broken chains; overly large κ magnifies ICE.

2 Error-Mitigation and Error-Correction Strategies

2.1 Spin-Reversal (Gauge) Transforms

For a random subset $S \subset \{1, \ldots, N\}$ we flip selected qubits and couplers,

$$h_i \;\mapsto\; (-1)^{\chi(i\in S)}\, h_i, \tag{3}$$

$$J_{ij} \;\mapsto\; (-1)^{\chi(i\in S)+\chi(j\in S)}\, J_{ij}, \tag{4}$$

where $\chi(\cdot)$ is the indicator function. Averaging over $g = 8$ gauges cancels first-order intrinsic-control error (ICE) bias with $\mathcal{O}(g)$ runtime overhead.

2.2 Logical Repetition Codes

Encoding one logical spin into $k = 3$ ferromagnetically coupled qubits rescales the logical energy by k and lowers the effective temperature. Majority-vote decoding yields a logical error rate $p_{\mathrm{L}} \approx p^2$ under independent bit flips.

2.3 Chain-Strength Optimisation

The ferromagnetic penalty λ must exceed the strongest logical coupling to prevent chain breaks, but not be so large that it compresses the problem Hamiltonian. A parameter sweep over $\lambda/J_{\max} = 8 \ldots 20$ revealed a clear optimum at

$$\boxed{\lambda/J_{\max} = 16}$$

for both raw embeddings and the Rep-3 code: break-fraction drops below 0.20 while best-cut values peak as in figure below. Increasing λ beyond 16 produced no further error reduction and slightly degraded cut quality due to energy-scale compression.

2.4 Anneal-Time Schedule

We sweep four dwell times $t_{\mathrm{a}} \in \{1, 5, 10, 20\}$ µs to trade off diabatic transitions (short ramps) against thermal excitations (long ramps). The best logical energies were invariably obtained at $t_{\mathrm{a}} = 10$ µs when combined with the optimal $\lambda = 16 J_{\max}$ and eight gauges (see Fig. **??**).

2.5 Nested Quantum-Annealing Correction (NQAC)

Iterating the repetition-code construction (*nesting level* k_{N}) produces an effective Hamiltonian with a minimum gap $\propto k_{\mathrm{N}}\Delta$ at the expense of k_{N}^2 physical qubits. We use $k_{\mathrm{N}} = 2$ and scale the chain strength linearly, $\lambda = k_{\mathrm{N}} \times 16 J_{\max} = 32 J_{\max}$, together with $t_{\mathrm{a}} = 20$ µs to exploit the larger gap.

3 Max-Cut Problem

Annealing is most suitable for optimization problems because the problem of finding a maximum or a minimum of a function naturally encodes in finding the ground state of the Hamiltonian corresponding to the given function.

To ground our study of quantum–error–correction (QEC) techniques, we employ the *Maximum-Cut* (Max-Cut) problem as a running example. Given an undirected, weighted graph $G = (V, E, w_{ij})$, Max-Cut seeks a bipartition $V = V_A \cup V_B$ that maximises the total weight of edges crossing the cut,

$$\max_{s \in \{\pm 1\}^{|V|}} \frac{1}{2} \sum_{(i,j) \in E} w_{ij}\big(1 - s_i s_j\big), \tag{5}$$

where $s_i = +1$ (-1) denotes vertex i assigned to V_A (V_B). Equation (5) is already quadratic, so it maps directly to an Ising Hamiltonian with zero local fields and pairwise couplings $J_{ij} = -w_{ij}/2$. Consequently Max-Cut can be programmed onto a D-Wave quantum-annealing QPU without auxiliary variables or higher-order reductions, making it an ideal vehicle for assessing hardware performance and the efficacy of QEC layers.

Max-Cut is pertinent to error-correction research for three reasons. **(i)** For small graphs, the ground-state energy is exactly known, and for larger instances, it can be tightly bounded, yielding an unambiguous success metric. **(ii)** Typical random or industrial graphs generate rugged energy landscapes with many near-optimal states, so thermal excitations, chain breaks, and control errors manifest clearly in the observed cut size and chain-integrity statistics. **(iii)** The logical encodings required by current QPUs are

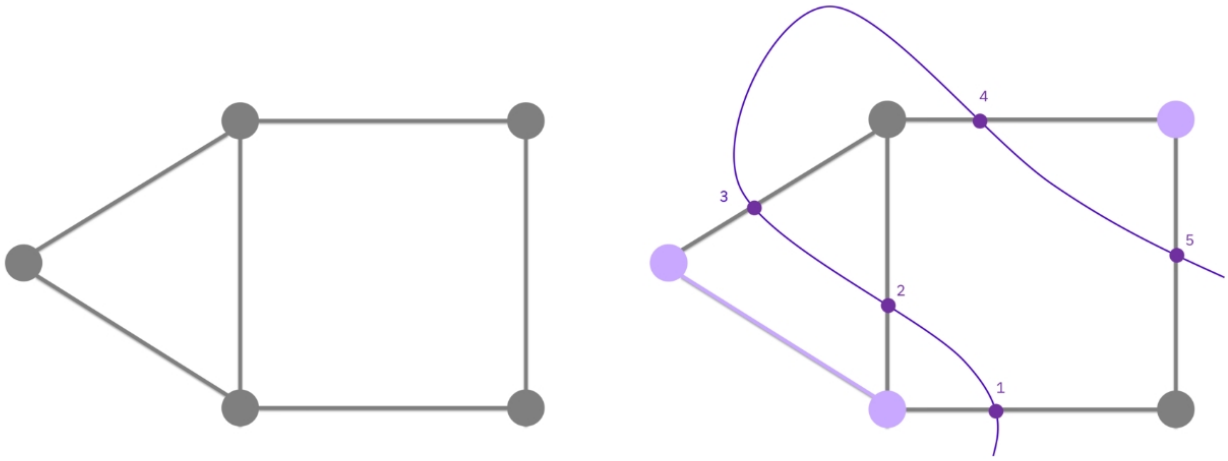

Figure 1: Max Cut Problem for a 5-node graph

simple: ferromagnetic chains realise minor embeddings, repetition codes repair broken chains via majority vote, and spin-reversal "gauge" transforms average out first-order calibration bias. By tracking improvements in best-cut value, energy depth, and average chain-break fraction under each mitigation layer, we obtain a quantitative measure of how well present-day QEC techniques enhance solution quality on quantum annealers.

4 Experimental Results

We benchmarked five sampling pipelines on a 50-node Erdős–Rényi graph ($p = 0.8$) whose optimal Max-Cut value, established by simulated annealing (SA), is 553. Table 1 summarises the best-observed cut size, corresponding energy, and average chain-break fraction for each method.

Table 1: Headline statistics over all runs (best instance per method).

Method	**Best Cut**	**Energy**	**Break-Frac**
Sim. Ann. (CPU)	553	−115	—
Raw QPU	526	−61	0.40
Gauge QPU	523	−55	0.44
Rep-3 (no gauge)	540	−2987	0.24
Rep-3 + 2 gauges	534	−3101	0.16

Relative to the raw embedding, spin-reversal gauges yield a modest improvement in best-cut quality, whereas the three-repetition code improves the best cut by ∼2.7% and reduces the chain-breaks by 40%.

4.1 Anneal-Time Dependence

Across anneal times $t_f = 1, 5, 10, 20\,\mu$s, raw and gauge pipelines saturate near $t_f = 5\,\mu$s. In contrast, *Rep-3* continues to improve up to $t_f = 10$–$20\,\mu$s, reaching a peak cut of 540, indicating that longer schedules particularly benefit logically encoded problems.

4.2 Chain-Strength Sweep

For repetition-encoded runs we varied the ferromagnetic chain strength $\kappa \in \{1.5, 2.0, 2.5, 3.0, 12, 14, 16\}$. Performance is bimodal: $\kappa \leq 3$ leaves chains fragile (break-frac >0.60), whereas $\kappa \geq 14$ both stabilises chains and deepens energies, with an optimum at $\kappa = 16$.

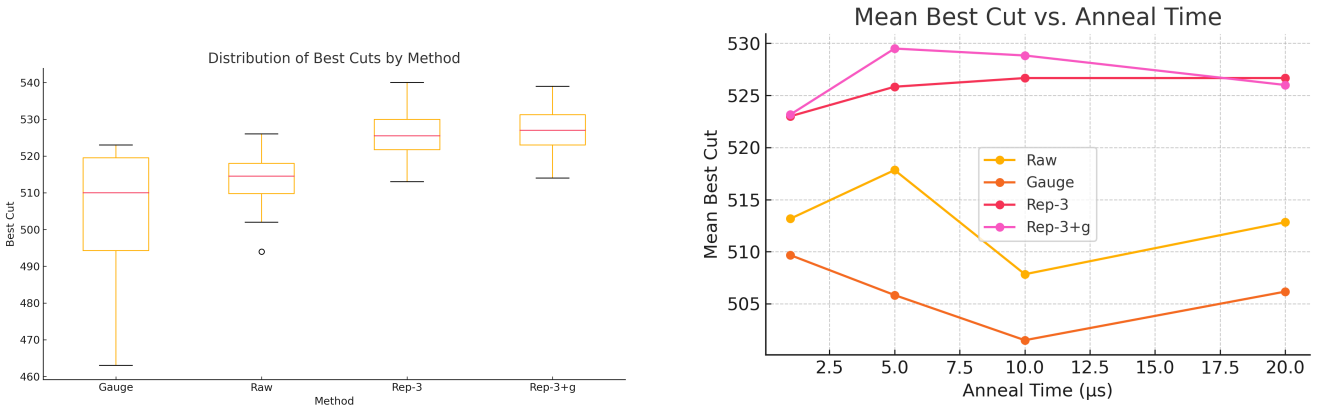

(a) Distribution of best cuts.

(b) Mean best cut vs. anneal time.

Figure 2: Performance comparison of mitigation layers.

5 Minor Embedding

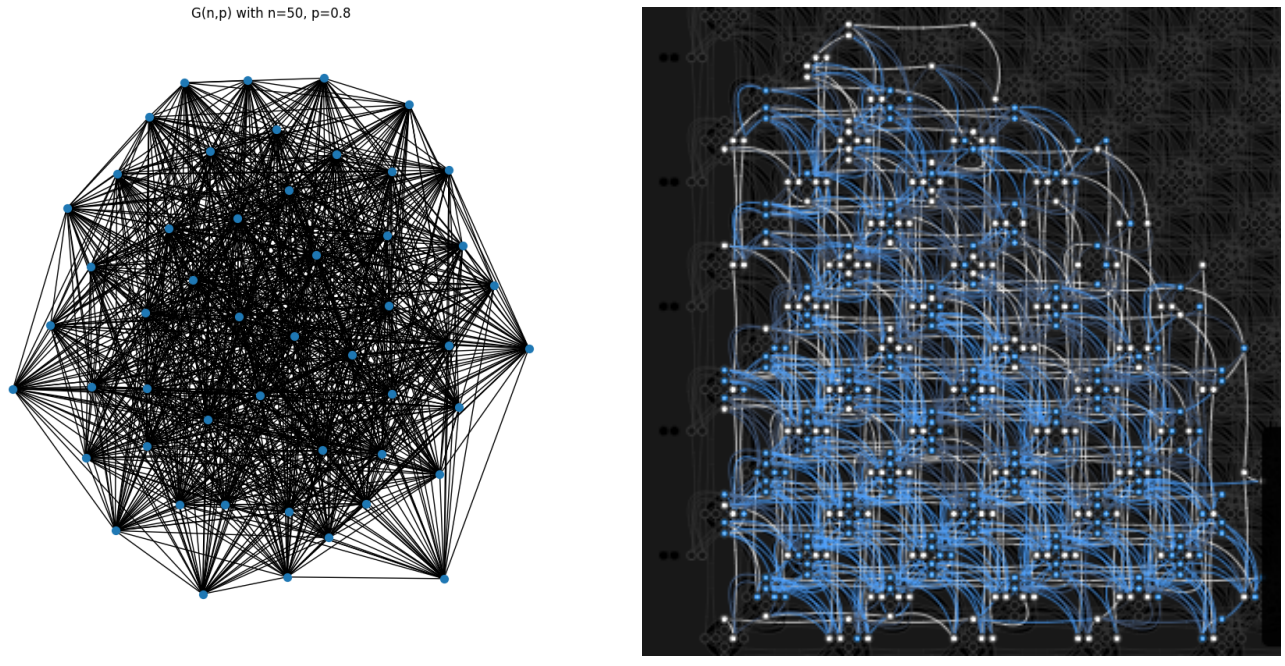

Figure 3: 50 node graph (a) and its corresponding minor embedding via qubit chains(b).

References

[1] K. L. Pudenz, T. Albash, and D. A. Lidar, "Error-corrected quantum annealing with hundreds of qubits," *Nature Communications*, vol. 5, p. 3243, 2014.

[2] K. L. Pudenz, T. Albash, and D. A. Lidar, "Quantum annealing correction for random Ising problems," *Nature Communications*, vol. 7, p. 1243, 2016.

[3] J. Marshall, V. Martin-Mayor, and I. Hen, "Analog errors in quantum annealing: doom and hope," *npj Quantum Information*, vol. 5, p. 52, 2019.

[4] M. Benedetti *et al.*, "Benchmarking quantum optimisation for the maximum-cut problem," *arXiv preprint*, 2024.

[5] E. Glauser, Z. Zhu, and H. G. Katzgraber, "Scaling advantage in approximate optimisation with quantum annealing," *Physical Review Letters*, vol. 134, p. 160601, 2025.

[6] A. D. King *et al.*, "Performance of quantum-annealing-inspired algorithms for Max-Cut," *Communications Physics*, vol. 7, p. 123, 2024.

[7] T. Stollenwerk and et al., "Benchmarking quantum annealers with near-optimal minor embeddings," *arXiv preprint*, 2024.

[8] A. Lucas, "Ising formulations of many np problems," *Frontiers in Physics*, vol. 2, p. 5, 2014.

[9] T. Kadowaki and H. Nishimori, "Quantum annealing in the transverse ising model," *Physical Review E*, vol. 58, no. 5, pp. 5355–5363, 1998.

[10] I. Hen, J. Job, T. Albash, T. F. Rønnow, M. Troyer, and D. A. Lidar, "Probing for quantum speedup in spin glasses," *Physical Review A*, vol. 92, p. 042325, 2015.

[11] K. L. Pudenz and D. A. Lidar, "Quantum annealing correction for degenerate ground states," *Quantum Information Processing*, vol. 15, pp. 3365–3380, 2016.

[12] T. Albash, V. Martin-Mayor, I. Hen, and D. A. Lidar, "Consistency tests of classical and quantum models for a quantum annealer," *Nature Communications*, vol. 7, p. 1246, 2015.

[13] D. A. Lidar, "Towards fault-tolerant adiabatic quantum computation," in *Quantum Error Correction*, pp. 649–676, Cambridge University Press, 2018.

[14] J. Preskill, "Quantum computing in the NISQ era and beyond," *Quantum*, vol. 2, p. 79, 2018.

[15] D-Wave Systems Inc., "D-Wave Documentation Portal: Ocean SDK and Quantum Annealing." https://docs.dwavequantum.com/en/latest/, 2025. Accessed 13 May 2025.